OPTIMIZATION OF THE GAS FLOW IN A GEM CHAMBER AND DEVELOPMENT OF THE GEM FOIL STRETCHER

Francesco NOTO[1,2], Valerie DE SMET[5], Vincenzo BELLINI[1,2], Evaristo CISBANI[3,4], Francesco LIBRIZZI[2], Francesco MAMMOLITI[1,2], Maria Concetta SUTERA[2]

[1]Dipartimento di Fisica ed Astronomia, Università di Catania, via Santa Sofia 64, 95123 Catania, Italy
[2] INFN - Sezione di Catania, via Santa Sofia 64, I-95123 Catania, Italy
[3]INFN - Sezione di Roma – Sanità group, P.le Aldo Moro, 2 I-00185 Roma, Italy
[4]Istituto Superiore di Sanità, viale Regina Elena 299, I-00161 Roma, Italy
[5]Haute Ecole Paul - Henri Spaak, ISIB, Brussels, Belgium

Corresponding Author: Francesco Noto, Dipartimento di Fisica e Astronomia, Università di Catania, Via Santa Sofia 64, I-95123 Catania, Italy. Email address: francesco.noto@ct.infn.it

The Gas Electron Multiplier (GEM) technology has been proven to tolerate rate larger than 50 MHz/cm^2 without noticeable aging and to provide sub millimeter resolution on working chambers up to 45x45 cm^2 [1]. A new GEM-based tracker is under development for the Hall A upgrade at Jefferson Lab. The chambers of the tracker have been designed in a modular way: each chamber consists of 3 adjacent GEM modules, with an active area of 40x50 cm^2 each [2]. We optimized the gas flow inside the GEM module volume, using the COMSOL physics simulator framework; the COMSOL-based analysis includes the design of the inlet and outlet pipes and the maximization of the uniformity of the gas flow.
We have defined the procedures for the assembling of the GEM modules and designed a mechanical system (TENDIGEM) that will be used to stretch the GEM foils at the proper tension (few kg/cm); the TENDIGEM is based on the original design developed at LNF [3].

Keywords: GEM foil, TENDIGEM, Fluid dynamic, Simulation, SBS Tracker

1. Introduction

In late 2014 the CEBAF electron beam at Jefferson Lab is expected to complete the energy upgrade to 12 GeV. JLab will become one of the most important experimental facilities for the study of the nucleon structure, in terms of form factors, transverse momentum distributions of the constituent partons and generalized parton distributions. New experimental equipment is under development for an optimal exploitation of the full potentiality of the new beam; a new hybrid tracker able to operate with luminosity as large as 10^{39} s^{-1}cm^{-2} is part of this development. The tracker will provide an average single hit resolution better than 80 μm and an event readout rate of about 20 kHz.

The tracker is made of two types of detectors: 40x50 cm^2 GEM modules and 10x20 cm^2 silicon microstrips. The former will be used as basic building blocks of large (~0.60 m^2) chambers that will seat behind a momentum analyzing spectrometer, while the latter will be positioned close to the scattering chamber, thus extending considerably the useful tracking arm. The hybrid design is aiming at a balance between cost and performance. The modular design of the GEM chambers (up to 6) intends to maximize reconfiguration on the existing or planned spectrometers of Hall A; each 40x50 cm^2 GEM module has its own high voltage supply and gas inlet/outlet as well as front-end electronics. Mechanics and gas flow have been investigated and optimized by Finite Element Analysis. The single module is made of 3 GEM foils and double layer x/y strip readout with 400 μm strip pitch. The modules are connected in a way to minimize the dead area and are supported by an external service frame.

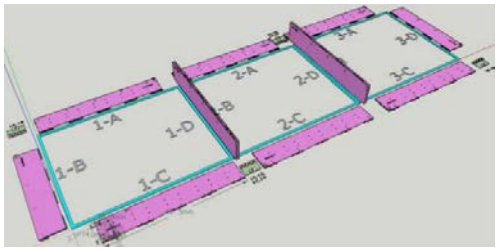

Figure 1: The triple GEM

2. Gas Input design

The role played by the gas mixture in the GEM detector is important. The avalanche process creates ions that pollute the gas degrading the performance of the detector. Thus the gas has to be constantly and relatively quickly replaced. The GEM structure being very thin, gas inlet and outlet pipes are limited in diameter. Hereafter we present a calculation of the minimal diameter of the pipes as a function of the rate of renewing. The characteristic number that measures the ratio between inertial and viscous forces is the Reynolds number:

$$Re := \frac{\rho V D}{\mu} \qquad (1)$$

where ρ is the density (expressed in kg/m^3), V is the gas velocity (expressed in m/s), D is the diameter of the pipe (in m) and μ the dynamic velocity of the gas (in Pa/s). If we denote by $\Phi = \pi D^2 V/4$ the flux of the gas (expressed in m^3/s), we obtain that, at fixed Reynolds number, the diameter of the pipe is given by:

$$D = \frac{4}{\pi} \frac{\rho \Phi}{Re\, \mu} \qquad (2)$$

To insure a laminar flow, the Reynolds number must not be greater than about 2300. With a mixture of Ar/CO_2 (70/30), and a renewing of the gas of 10 times per hour, we find for the 10 cm x 10 cm test detector (using ρ = 1.7 kg/m^3 and $\mu = 2\times10^{-5}$ Pa/s and a thickness of 9 mm) a minimum diameter of 3×10^{-4} mm.

The diameter will vary linearly with the dimensions of the detector and with the rate of refreshing of the gas, and in inverse proportion to the viscosity of the gas. It will also depend on the temperature as the density decreases as T^{-1}, while to first approximation the dependence of the viscosity on the temperature is given by the Sutherland empirical law:

$$\mu = \mu_0 \frac{T_0 + C}{T + C} (T/T_0)^{3/2} \qquad (3)$$

Here C is the Sutherland's constant, which depends on the nature of the gas and is of the order of 200 (C_{Ar}=144; C_{CO2}=240). To first approximation the computed diameter will behave like $(T_0/T)^{5/2}$ as a function of the temperature, and thus will vari by a factor of the order of 0.9 between 15 °C and 25 °C. Another parameter that must be taken into account is the dependence of the flux on the diameter of the pipe, $\Phi \propto D^4$ in laminar regime, but this effect can be compensated by adjusting the pressure gradient. This dependence of the flux on the diameter of the pipes justifies its optimization.

2. Simulation

Permanent gas flow in a module is required to provide the expected gain and signal timing, to evacuate gas that contaminates the mixture and to prevent fast aging of the detector due to radiation-induced chemical reactions in the gas. The gas flow should be spatially uniform in order to guarantee a homogeneous and stable detector response. Therefore, the goal of our study was to optimize the design of the frame separating two GEM foils in order to obtain the optimal gas flow uniformity over the active area of the module.

3. Use of Finite Element Method

The Finite Element Method (FEM) approximates a Partial Differential Equations problem with a discretization of the original problem based on a mesh, which is a partition of the geometry into small units of simple shape called mesh elements. The FEM method looks for a solution in the form of a piecewise polynomial function, each mesh element defining the domain for one "piece" of it. Such a piecewise polynomial function will be expressed as a linear combination of a finite set of predefined basis functions. Let us consider for example a 2-dimensional problem with a single dependent variable p(x,y). We would like to solve this problem based on a mesh with quadratic triangular elements. The expression "quadratic elements" refers to the fact that on each mesh element the sought piecewise polynomial function $p^*(x,y)$ is at most a quadratic polynomial. In this case, the solution is expressed as:

$$p\,(x,y) \cong p^*(x) = \sum_{i=1}^{n} p_i \varphi_i(x,y) \qquad (4)$$

where i refers to a node of the mesh, p_i are the degrees of freedom, $\varphi_i(x,y)$ are the basis functions and n is the total number of nodes, under the assumption that each triangle of the mesh possesses six nodes: three corner nodes and three mid-side nodes [4]. A basis function $\varphi_i(x,y)$ has here the restriction to be a polynomial of degree at most 2 such that its value is 1 at node i and 0 at all other nodes [5]. The degree of freedom p_i is thus the value of $p^*(x,y)$ at node i. The definition of the basis function associated to each node of the mesh can be derived using for example a general method introduced by Silvester in 1969 [6].

3.1. Simulations development

All the details on the selection of the physical parameters in the design of the GEM are taken from ref. [5].

The geometry of the frame separating two GEM foils has been constructed in 2 dimensions, whereas the third dimension, which corresponds to the gas film thickness, has been inserted as a parameter of the physical model. Actually, two separate Thin-Film Flow models have been defined in order to account for the two different film thicknesses in the problem: 2 mm in between two GEM foils and 1 mm inside the openings of the frame's spacers and inside the inlets and the outlets.

As far as the inlets and outlets are concerned, it has not been possible to define their exact configuration, because this requires to use a physical model that can be applied to a geometry constructed in 3 dimensions. Therefore, we have defined inlets and outlets as 8x5 mm rectangular zones with a uniform film thickness of 1 mm.

Typical flow in gas detectors corresponds to ⅓ volume renewals per hour. If the 3 GEM modules of one chamber are connected to each other in series with respect to the gas flow, the total gas volume for a 2 mm thick "floor" of the chamber is approximately $3 \cdot 0.4 \cdot 0.5 \cdot 0.002 = 0.0012$ m^3, so ⅓ volume renewals per hour correspond in our case to a gas flow between 20 cm^3/min and 60 cm^3/min. Nearly all our simulations have therefore been made with a total flow of 60 cm^3/min imposed at the inlets. In a frame with 2 inlets, each having a cross-section of 8 mm^2, the mean entrance velocity is then U_e = 0.0625 m/s. If one wants to evaluate whether such a stationary gas flow is incompressible or not, the mean velocity should be compared to the speed of sound in the same medium [4]. For an ideal gas, the speed of sound is given by the following formula:

$$U_s = \sqrt{\frac{\gamma R T}{M}} \qquad (5)$$

where γ is the adiabatic constant of the gas, R = 8.314 J/(mol·K) is the universal gas constant, T is the temperature and M is the molecular mass of the gas. In our case, we consider that $\gamma \approx 5/3$ since argon is the main component of the gas mixture; T = 293 °K and $M \approx 0.70 \cdot 0.03995 + 0.30 \cdot 0.04401 = 0.04117$ kg/mol. For the speed of sound, we thus obtain $U_s \approx 314$ m/s >>> U_e = 0.0625 m/s. Therefore, it has been assumed that the gas flow is incompressible and a constant value for the density ρ has been used. Somehow, it is useful to get rid of the density's dependence on the pressure. The ambient pressure p_a has been set to 1 atm. However, the solution for the velocity field does not depend on this value. The obtained velocity field does not depend either on the value of the constant density ρ which, for a Ar-CO_2 (70/30) mixture at 20 °C and 1 atm, can be computed using the densities at 20 °C and 1 atm of respectively argon and carbon dioxide (ρ_{Ar} = 1.7837 kg/m^3 and ρ_{CO2} = 1.9770 kg/m^3), with the following formula:

$$\rho = \left(0{,}30 \cdot \rho_{CO_2} + 0{,}70\rho_{Ar}\right) = 1{,}8417\,\frac{kg}{m^3} \qquad (6)$$

To compute the dynamic viscosity at 20 °C and 1 atm of the gas mixture, we have used the Reichenberg's formula [7] with parameters from literature and we have obtained:

$$\mu = 1.9696 \cdot 10^{-5}\ \text{Pa·s} \qquad (7)$$

In the two defined Thin-Film Flow Models, instead of considering two moving solid structures, we have forced the normal displacements, Δh_m and Δh_b, and the tangential velocities, u_m and u_b, of these structures to zero, so that the film thickness h would remain constant at its initial value h_0. We have also assumed in the first place that the fluid can be treated as a continuum. Actually, the Knudsen number obtained with our no-slip models was around $5 \cdot 10^{-5}$, which is indeed negligible with respect to 0.1.In our case, the ambient pressure p_a has been set to 1 atm. As boundary conditions:

- We have imposed a uniform perpendicular velocity (e.g. 0.0625 m/s) on the external 8 mm side of the inlets.
- On the external 8 mm side of the outlets, we have forced the additional pressure p_f to zero.
- "Walls" have been inserted on the sectors of the geometry that represent surfaces of the frame. This imposes the standard wall boundary condition $\overrightarrow{U} = \vec{0}$ on these sectors.

When simulating a system that is quite complex, it's advisable to start with a strongly simplified geometry and increase progressively the complexity of the model, as one's understanding of the simulation improves [4]. We have started by simulating a frame with only two sectors, separated by a spacer containing just one opening of length 15 mm. One inlet (with velocity 0.0625 m/s) and one outlet have been defined. The problem has been treated as stationary and a predefined mesh type of COMSOL ("Normal") has been used, which in our case is made up of 24182 unstructured quadratic triangular elements. The obtained velocity field is shown in Figure 2.

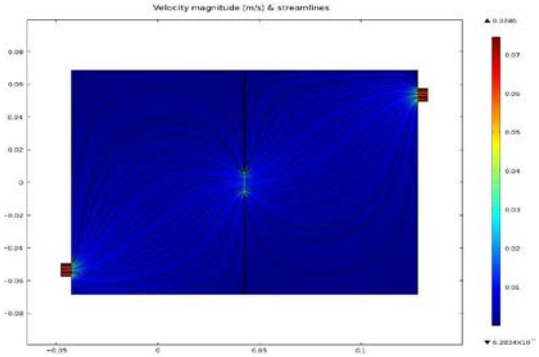

Figure 2: Velocity magnitude on a linear scale and streamlines of the velocity field obtained in the case of a frame with 2 sectors, 1 inlet at the left and 1 outlet at the right. The two sectors communicate through a central opening of 15 mm.

In a next step, we have simulated six adjacent sectors of the frame and included two 15 mm openings in each spacer. It has been useful to define a time-dependent model in which the inlet velocity increases smoothly from 0 to 0.0625 m/s. We are however not mainly interested in this evolution and we focus on the results obtained for the final state (Figure 3). In this simulation, we have also tried out a more complex mesh, consisting of a predefined "Fine" unstructured quadratic triangular mesh in the central regions (133276 elements) and a "Boundary Layer", made up of parallel rectangular quadratic elements along the borders of the geometry (39252 elements). Note that on Figure 3, the scale has been cut at a tenth of the maximum velocity.

Based on these results, we have tried to modify some aspects of the frame's design in order to reduce, in number and/or in size, the zones with particularly high or low velocities. The optimization of the frame design has been realized by gradually modifying the simulated geometry and comparing each time the new results with those from previous simulations.

In all our simulations of full-sized frame versions, we have used the time-dependent model but without working with the same type of mesh as in the six-sectors simulation, because of the too large number of elements (over 500000).

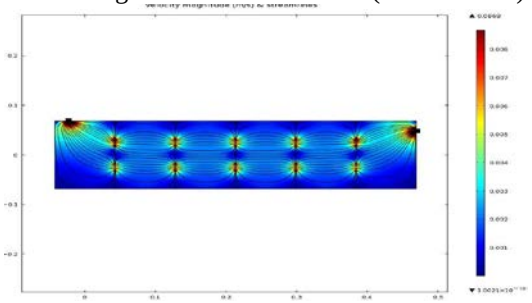

Figure 3: Velocity magnitude on a linear scale and streamlines of the velocity field obtained in the case of a frame with 6 sectors, 1 inlet (left) and 1 outlet (right).

We have defined another type of customized mesh consisting of three predefined unstructured quadratic triangular mesh types:

- in the inlets and outlets, as well as in a 16 x 10 mm^2 rectangular zone in front of each of them, we have defined a "Finer" ("Extremely fine") mesh, in the first two (last four) simulations.
- in the central openings we have defined a "Fine" ("Extra fine") mesh, in the first two (last four) simulations.
- in the rectangles left over in the center of the several frame sectors, we have defined a "Normal" ("Finer") mesh, in the first two (last four) simulations.

Furthermore we have perfomed all six simulations using either 15 mm or 20 mm thicknesses for the central openings.

In this way, we have tried to refine our meshes without exceeding 250000 elements. Since the geometry is different in each simulation, in order to assess in some way the precision of our different simulations we have compared for each simulation the inlet and the outlet total fluxes based on the computed velocity field. Since the flow is supposed to be conserved, these fluxes should in theory be equal and, of course, correspond to the initially imposed value (e.g. 60 cm^3/min).

3.1.1 Analysis and results

3.1.1.1 Simulation 1: Full frame in its first prototype version

In its first prototype version, the frame separating two GEM foils possesses 18 sectors, 2 inlets and 2 outlets. Two adjacent sectors along the longest side of the module communicate through 2 openings of 15 mm, while two adjacent sectors along the other direction communicate through a single 15 mm opening. In our simulation, the uniform velocity imposed on both inlets is 0.0625 m/s, which corresponds to a total flow of 60 cm^3/min. Note that the scale has been cut at a tenth of the maximum velocity. A contour plot with logarithmic scale of the velocity magnitude is also given in Figure 4.
As expected, the zones with lower velocities are found mainly in corners where spacers cross each other or reach the border of the frame, and in the four corners of the outer structure of the

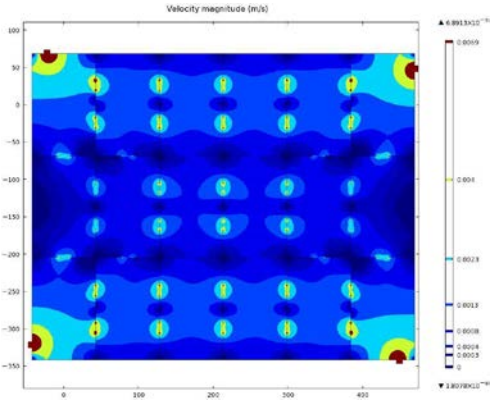

Figure 4: Simul. 1 – Contour plot with logarithmic scale of the velocity magnitude obtained in the case of the full frame in its first prototype version.

frame. However, our attention has also been drawn towards two large low-flux zones at the extremities of the central 6-sectors row, which contains no inlets and outlets. For this reason, in our next simulation we included an extra inlet and outlet, placed at the level of this central row. Zones with higher velocities correspond to inlets, outlets and openings in the spacers, especially in the spacers parallel to the shortest side of the module. Figure 5 shows a close-up on one of the inlets. Although our simulation isn't the most appropriate to estimate the actual velocity field in the region of inlets and outlets,

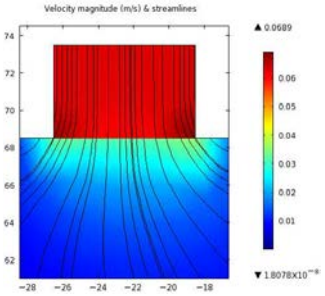

Figure 5: Simul. 1 – Velocity magnitude on a linear scale and streamlines of the velocity field obtained for one of the two inlets in the first prototype version.

we can realize from it that the 90 degree angles between an inlet (or outlet) and the borders of sectors are responsible for particularly high velocities, which are in fact also much higher than in the openings of spacers (Figure 6). The maximum velocity computed by the simulation (0.0689 m/s) is indeed found on these edges at the inlets and outlets. Thereupon, we decided also to replace in our next simulation these 90 degrees edges by circular joints of radius 1.5 mm.

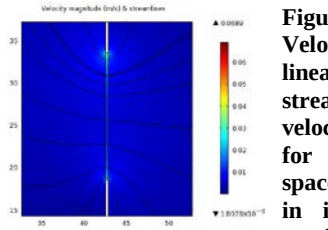

Figure 6: Simul. 1 – Velocity magnitude on a linear scale and streamlines of the velocity field obtained for an opening in a spacer of the full frame in its first prototype version.

3.1.1.2 Simulation 2: Modifications to the inlet and outlet configuration

In this second simulation, one inlet and one outlet have been added with the aim to improve the uniformity of the gas flow in the central 6-sectors row of the frame. The exact positions of these inlet and outlet have been selected based on the available space in the detector. For all inlets and outlets, the aforementioned circular joints of radius 1.5 mm have also been introduced. The 60 cm^3/min flow has been

maintained, resulting in an inlet velocity of 0.04167 m/s. In Figure 6, the obtained velocity magnitude is shown on a linear scale (cut to a tenth of the maximum velocity), together with the streamlines. Figure 8 is a contour plot of the velocity magnitude with a logarithmic scale. On a qualitative basis, the overall uniformity of the velocity magnitudes looks improved by the added inlet and outlet. It seems that in this configuration we obtain in the six-sectors rows three relatively independent and similar flows. In order to show the effect of the circular joints at inlets and outlets (cf. Figure 8), we have also run the same simulation using the initial geometry of the inlets and outlets.

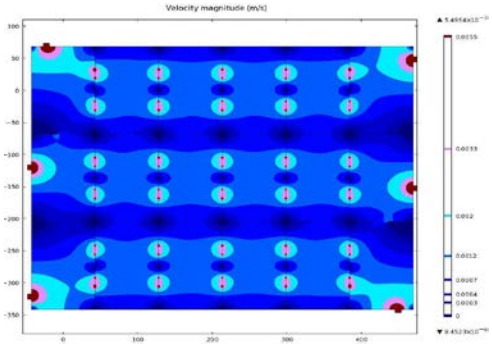

Figure 7: Simul. 2 – Contour plot with logarithmic scale of the velocity magnitude obtained for an 18-sectors frame with 3 inlets (left) and 3 outlets (right).

Figures 9 and 8 share the same color scale, so that the slight reduction of the high velocities inside the sector is visible in the design with circular joints. It will help avoiding their separation from the walls and thus avoiding possible small turbulence areas near the inlets and outlets.

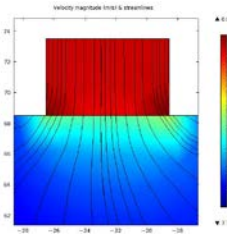

Figure 8: Simul. 2 bis – Inlet without circular joints

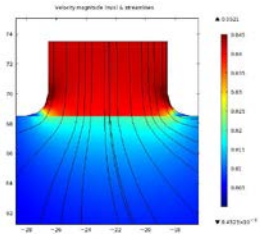

Figure 9: Simul. 2 – Inlet with 1.5 mm radius circular joints

3.1.1.3 Simulation 3: Reduction of the number of sectors from 18 to 12

Since low velocity zones are found where spacers intersect each other or reach the border of the frame, reducing for example the number of spacers would be a way to reduce these "stagnation" zones, which might thus improve the overall uniformity of the gas flow. A sector of a GEM-foil glued to its frame can be modeled as a built-in rectangular thin plate of area S, being isotropically stretched by a uniform force per unit length T at its circumference, and undergoing a normal pressure P. The maximum deformation u_{max} of such a plate is given by the following expression:

$$u_{max} = k\,(\zeta) = \frac{PS}{T} \qquad (8)$$

where the geometrical factor $\kappa(\zeta)$ is an increasing function of the ratio $\zeta \in]0, 1]$ of the rectangle sides. For a square plate, κ reaches a maximum value of nearly 0.074. In our case, we want the maximum deformation u_{max} to remain lower than 1% of the 2 mm thick gap between two GEM-foils, at a pressure P up to 10 N/m^2, when a tension of 1 kg/cm (T = 9.81 N/cm) is applied to the GEM-foil. If we consider in first approximation a geometrical factor κ of 0.074, the maximum allowable area S of a sector should thus be:

$$S = \frac{u_{max}T}{kP} = \frac{2 \cdot 10^{-5} \cdot 9.81 \cdot 10^{2}}{0.074 \cdot 10} = 2.65 \cdot 10^{-2} m^2 \qquad (9)$$

Based on these assumptions, it would have been feasible to reduce the number of sectors to only 9 (using 2 spacers along both directions), since the area of each sector would have been equal to $\frac{0.2}{9}\ m^2 = 2.22 \cdot 10^{-2}\ m^2$. However, a more conservative choice of 12 sectors (2 spacers along the long side and 3 spacers along the short one) has been made, which results in sectors of about 0.125 x 0.133 m^2 = 1.66 · 10^{-2} m^2. In the simulation results for a frame with 12 sectors, the overall uniformity of the gas flow seems indeed improved by the reduction of the number of spacers along the shortest side of the module.

3.1.1.4 Simulation 4: Enlargement of some openings in the spacers

With the hope to further improve the flow uniformity, especially in the sectors possessing an inlet or an outlet, we have made a simulation in which the openings in the spacers that delimit these particular sectors are enlarged from 15 to 20 mm. The results have however not been so

convincing. For this reason, the idea of modifying the width of the openings in spacers has been abandoned.

.

3.1.1.5 Simulation 5: Nine openings in the spacers along the short side of the module

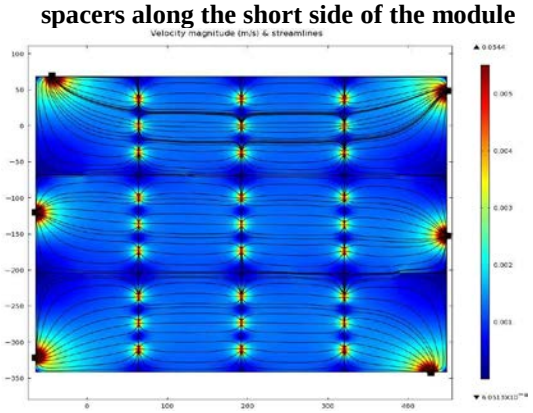

Figure 10: Simulation 5 – Velocity magnitude on a linear scale and streamlines of the velocity field obtained for a 12-sectors frame with 3 inlets (left) and 3 outlets (right), having nine 10 mm openings in the spacers along the short side of the module.

Good results have been obtained with nine openings of 10 mm instead of six openings of 15 mm for the spacers along the short side of the module. When comparing Figure 10, with the figures from previous simulations, we notice a reduction in size of the low velocity zones where spacers cross each other and where the short spacers reach the longest border of the frame.

3.1.1.6 Simulation 6: Doubling the openings in the spacers along the long side of the module

After the results of Simulation 5, we have tried to find out whether doubling the number of 15 mm openings in the spacers along the longest side would decrease the size of the large low velocity zones near the shortest borders of the frame. However, these long spacers are parallel to the main direction of the gas flow, instead of being perpendicular to it like the short spacers.
For this reason, increasing the number of openings in the long spacers does not produce the same positive effect on the flow uniformity.
We have therefore decided to stick with the frame design of Simulation 5, since in Simulation 6 we have not found a sufficient improvement of the flow uniformity to justify

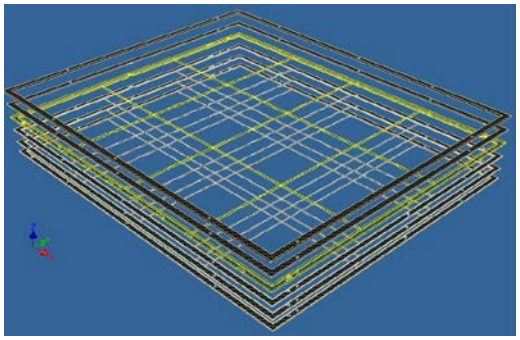

adding openings in the long spacers and thus weakening the mechanical support they provide.
Figure 11: All frames of the module assembled

The finally chosen new frame designs is the one yielding the simulations results shown in figure 10.

4. TENDIGEM TENSION CONTROL SYSTEM

TENDIGEM is a tool designed to stretch a GEM-foil before gluing it to the frame that will hold the foil. This tool is a sensor-based device which uses load cells to measure the tension. The load cells of the TENDIGEM monitor the tension on the different sides of the foil. It is important to stretch the foils properly because if a GEM foil shrivels, it can touch another foil. So when the foils are not stretched properly, there is a big chance that an electrical short will occur in the foil, which would make the detector useless.
The GEM-foil will be placed in the TENDIGEM by using the clips that are provided. There are 14 clips in total as shown in fig. 11. Only half of the clips are connected with the load-cells. After a foil is correctly stretched, the frame will be glued on it. Fiducial metal pins located on the sides of the TENDIGEM and corresponding holes in the frames are arranged asymmetrically in order to easly match the appropriate sides of either one. The frame is then glued with polymeric glue to the GEM-foil and allowed to dry for 24 houres.
Once the glue has dried they are removed from the TENDIGEM. At this point the frame and foil are ready to use in a GEM-chamber.
To improve the GEM detector assembly method an electronic control system is used. In the TENDIGEM the goal is to create the correct tension on a GEM-foil before it is glued to the frame.
There are different ways to put tension in a controlled way on a system, like Sensor Based Tension Control or Open Loop Tension Control. The Sensor Based Tension Control uses load

cells that measure the tension in a point and compare it with the desired tension level. If it is necessary the load cells will induce the controller to do some adjustments. This is an example of a closed loop control system and has an accuracy of 1-2%. In an Open Loop Tension Control System there is no feedback. The system only estimates what the value at the output will be. The accuracy for an Open Loop Tension Control System is 8-10%. In the TENDIGEM the system used is Sensor Based Tension Control (Fig.12) that uses load cells.

5. CONCLUSION

Our goal has been to obtain a better spatial uniformity (over the active area of the module) of the continuous Ar-CO_2 (70/30) gas flow in the 2 mm gap between two GEM foils, since this gas flow should be spatially uniform in order to guarantee a homogeneous and stable detector response. With a frame geometry defined in two dimensions, we have used the built-in Thin-Film Flow Model, which treats the laminar and isothermal flow of a thin fluid film between two large solid structures and solves the corresponding Reynolds equation. We have defined a typical total gas flow of about 3 chamber-volume renewals per hour (60 cm^3/min) and this gas flow has been considered incompressible. The optimization of the frame design has been presented through six main simulations, showing incremental modifications of the simulated geometry. The initially defined geometry corresponds to the first prototype version of the frame, possessing eighteen sectors, two inlets and two outlets. A second simulation has shown that adding a third inlet and a third outlet improves the overall flow uniformity, as the flows in the three six-sector rows become rather independent and similar. High velocity zones near inlets and outlets have also been reduced by replacing 90 degrees edges with 1.5 mm radius circular joints. In a third simulation, the number of stagnation zones has been decreased by reducing the number of short spacers from five to three, leading to a frame with twelve sectors which still meets the mechanical requirements related to the planarity of the GEM foils. The fourth simulation, in which openings in the spacers near the inlets and outlets have been enlarged from 15 mm to 20 mm, has not yielded a significant improvement of the gas flow uniformity. However, the fifth simulation has shown that introducing in the short spacers nine openings of 10 mm, instead of six openings of 15 mm, decreases the size of various stagnation zones. Finally, we have concluded from a sixth simulation that doubling the number of 15 mm openings in the long spacers does not significantly improve the flow uniformity and thus the geometry of the fifth simulation has been selected as the basis for a new frame design.

Figure 12: The TENDIGEM Tension Control System

6. REFERENCES

[1] M. Alfonsi et al " Activity of CERN and LNF groups on large area GEM detectors" Nucl. Instr. Meth. A 617 (2010) 151.

[2] J. Alcorn et al - "Basic instrumentation for Hall A at Jefferson Lab", Nucl. Instr. Meth. A 522 (2004) 294.

[3] G. Bencivenni, "The GEM detector activity at the Frascati Laboratory," Nucl. Phys. A 827 (2009) 614C1. Author, Article title, *Journal*,

[4] Felippa C.A., Introduction to Finite Element Methods, lecture notes, Department of aerospace engineering sciences of the University of Colorado, Boulder, 2004.

[5] COMSOL Multiphysics User's Guide v4.1, COMSOL A B, 2010.

[6] Lewis R.W., Nithiarasu P. & Seetharamu K.N., Fundamentals of the Finite Element Method for Heat and Fluid Flow, New York, John Wiley & Sons, 2004.

[7] Alfonsi M. et al., Aging measurements on triple-GEM detectors operated with CF_4-based gas mixtures,Proceedings of the 9th Topical Seminar on Innovative Particle and Radiation Detectors, Nucl. Ph. B – Proceedings Supplements, Vol. 150, pages 159-163, BIBLIOGRAPHY 119 January 2006.